

TEM of epitaxial thin films controlled by planes extending (near) normal to interface; with application to two methods to reduce crystal orientations in polycrystalline magnetic media

Warren MoberlyChan^{a,*}, Paul Dorsey^b

^aCenter for Imaging and Mesoscale Structures at Harvard University, Cambridge, MA 02138, USA

^bGeneral Electric, Inc., 1704 Automation Parkway, San Jose, CA 95131, USA

Abstract

This work is a study of heteroepitaxial interfaces as applied to multilayer-thin films for magnetic information storage media. With a goal to develop a film crystallography that optimizes the alignment of magnetic dipoles to coincide with the write/read signal of the recording head, two TEM observations have elucidated a better understanding of what controls heteroepitaxial interfaces. The classical approach to establishing “lattice matching” of interfaces is to model the top plane of atoms of the substrate and then align the next plane of atoms in the subsequently deposited film, i.e. plane A and plane B should “match” (with minimal misfit), with both planes being parallel to the interface. Such mechanism is valid for idealized slow MBE growth where the planes remain atomically flat. However, most film deposition conditions quickly violate this atomically flat configuration. Here growth on a roughened interface is shown to be controlled by the matching of planes that extend (normal or near-normal) across the interface. A second classical observation is the nucleation of bi-crystals, which naturally increases the number of crystal orientations in subsequent films. However, this work exhibits two cases of reducing orientations! One case has a 3-D isotropically oriented cubic film followed by a hexagonal film with 2- $\frac{1}{4}$ -D isotropy, and a second case where a 2-D random cubic film is followed by a hexagonal film with 1- $\frac{1}{2}$ -D isotropy. The understanding and control of these heteroepitaxial interfaces enables reduction of film orientations to enhance properties, such as 100 Gigabit per-square-inch magnetic recording.

© 2003 Elsevier Ltd. All rights reserved.

Keywords: Co; Cr; Epitaxy; Magnetic recording media; NiAl; Oriented thin films; TEM

1. Introduction

The nucleation and growth of thin films depend on each film's crystallographic relationship to previously deposited layers. TEM and Electron Diffraction are used to characterize the interfacial dependence between multiple layers of ion-sputter-deposited films, as well as to elucidate how film growth processes can be controlled to produce specific material properties. The specific films considered in this study are the layers comprising magnetic storage media in a hard drive. The mechanisms in the hard drive include a recording head flying above a spinning disk, and this design requests

the magnetic dipoles in the stored longitudinal media to be pointing in a circumferential direction.¹ This in turn requests the crystallography of the magnetic layer to ideally have the dipoles with 1-dimensional texture and preferentially aligned in the circumferential direction in the plane of the film. Top-down template models are often coupled with out-of-plane XRD to understand heteroepitaxial interfaces; however, this work also uses plane-view electron diffraction coupled with models of planes extending between layers to understand reduction of crystallographic orientations in succeeding films. Controlling magnetic properties in media films requires control of crystallography and microstructure in the seed layer(s), as well as the control and understanding of the interfacial relationships.

The interfaces between thin films establish the orientation relationship between such films; with the hope that by controlling the orientation of the lower (seed)

* Corresponding author. Tel.: +1-617-496-8832; fax: +1-617-496-4654.

E-mail address: moberlychan@deas.harvard.edu (W. MoberlyChan).

layer one can in turn control the orientation of the subsequently deposited upper layers. In the simplest of thin film growth, such as an MBE system, an epitaxial or heteroepitaxial film can be grown on a single crystal substrate, ideally keeping a single crystal orientation in the film (plus or minus a few misfit dislocations at the interface). A common approach to viewing thin film growth is to view the surface plane of the substrate and then to template the first atoms deposited of the thin film to match the locations of atoms in the surface plane of the substrate,^{2,3} e.g. considering a substrate crystal with plane stacking of ABAB, and terminated with a surface layer of “B”, the first layer of the thin film will wish to be A. And if this 1st plane of the thin film successfully deposits its atoms as “A”, then the thin film growth is essentially insured to have a single crystal orientation, the same as the substrate. It still remains possible, however, that the crystal structure of the film may become different than that of the substrate. For example, if the ABAB substrate is followed by ABCABC, an FCC film has been grown on a HCP substrate, but still with a singular orientation as controlled by the interface layer. This orientation relationship naturally has inversion symmetry, which means if the system is turned upside-down, then an ABAB film would grow on an ABCABC substrate.

It is possible, of course, that something can go wrong (contamination, defects and/or severe lattice mismatch), such that the film does not develop the correct and singular orientation. One simple mistake can be the statistics of nucleation, where the thin film nucleates differently in different locations on the substrate. Continuing the above simple case, in one region the film may nucleate ABCABC, whereas in another region the film may nucleate CBACBA. In so doing, the thin film will develop as a “bi-crystal”, with two orientation relationships between film and substrate, depending on location in the film.^{4,5} This problem of statistics, and especially contamination problems, will commonly lead to more orientations present in the thin film (i.e. polycrystalline film) than the single crystal of the substrate. Although the orientation relationships between a bi-crystal film and a single crystal substrate remain valid when turned upside-down, the growth of a single crystal film onto a bicrystal or polycrystalline substrate has not been experimentally observed. Thus the development of thin film materials with less orientations than their underlayers represent an important goal in thin film processing and requires judicious control and understanding of interfaces.

This work considers thin films grown to provide optimal magnetic properties for recording media in a hard drive.^{1,6} Although the hard drive has miniaturized over the past two decades (while increasing storage capacity from 100s of kilobytes to 100s of gigabytes), it

has remained a mechanical-magnetic device known as the Winchester architecture. Fig. 1 exhibits a spinning disk that has a magnetic coating that stores the information,¹ and a read/write sensor (head) flies just above the surface on an arm (akin to a phonograph except with fast random access). A critical mechanical or aerodynamic aspect is that the spinning disk influences the air pressure that causes the head to “fly”. The critical aspect of ever-higher recording density requires not only shrinking the sensor, but also reducing the flying height to <20 nm. The mechanical-magnetic relationship has been symbiotic; for example, the magnetic requirement of ever-closer fly height has altered the read/write head from positive to negative pressure aerodynamics. And the introduction of scratches on media surfaces to inhibit head stiction during start/stop operations has in turn developed a media with enhanced magnetic recording geometries.

The read/write head is essentially a horseshoe magnet, albeit an electromagnet miniaturized by thin film processing. The write gap in the miniature horseshoe magnet leads to a field passing through the nearby media, and an ideal media would have a crystallographic orientation that eases the alignment of dipoles in this longitudinal (in-plane), and circumferential direction. Because of a need for high coercivity for stable magnetic storage, Co–Pt-alloy thin films have developed as the medium of choice even though size and substrates vary in different drive applications. The fine polycrystalline microstructure of sputter-deposited Co also enables magnetic isolation between storage bits without a lithographic patterning. However, as media bits are written around the disk in a circular pattern, the ideal crystal structure would be to have each grain of Co grown in the film such that its hexagonal *c*-axis is aligned circumferentially. This would enable the crystallographic dipole of each grain to match the dipole directions of the read/write sensors. An *x/y* coordinate system or hexagonal symmetry is easily achieved on single crystal Si platforms, but a method of thin film deposition that produces grain orientations only in the circumferential direction is not easily imagined.

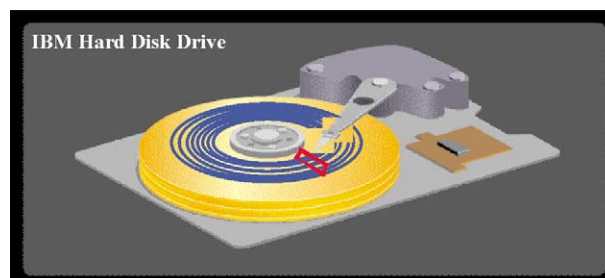


Fig. 1. Schematic of Winchester hard drive¹ with scratches on longitudinal media in the circumferential direction that head writes/reads.

2. Experimental results and discussion

2.1. Co-alloy/Cr/scratched-Ni(P)-substrate; reduction from 2-D-isotropy to 1-&1/2-D

Fig. 2 is a schematic cross section of the thin films on the media substrate in a typical computer hard drive. This view is in the circumferential direction, which means the write/read sensor would be producing a field in the media film normal to this diagram. Also shown is a set of texture scratches in cross section, where these scratches prevent the head from sticking to the substrate, as would happen for flat surfaces. These circumferential scratches are applied to a polished substrate (with a present-day roughness R_a of only a couple nm and spaced 10s of nm), and this scratch roughness is carried through to each subsequently sputter-deposited seed layer(s), magnetic media layer, and overcoat(s). As is common to other thin film processes, a “seed” layer (or multiple sequential seed layers) is (are) grown beneath the Co layer of interest. The first goal of the seed layer is to provide a crystallographic template that enables the Co film to grow with its hexagonal (c) axis in plane, defined as longitudinal media. (Additional goals of the seed layer would be to limit grain size and thus enable smaller magnetic bits for higher density recording; to potentially affect thin film stress that may enhance mechanical durability and/or magnetostrictive properties; and to serve as a diffusion or corrosion barrier which prevents reactions with the substrate.) As drawn schematically in Fig. 2, the dipoles would expectedly be oriented randomly in 2-D within the film of Co. However, ideal magnetic properties request each crystalline dipole to be aligned circumferentially to match the dipole written by the head.

Fig. 3a (courtesy of T. Nolan⁷) exhibits a HR-TEM (high resolution transmission electron microscope) lattice image of the bicrystals of Co that make up the magnetic media in a typical storage hard drive. In this plan-view sample (thinned from the back side), the Co

exhibits a $\langle 11\bar{2}0 \rangle$ orientation, and this is achieved by depositing on a [200] Cr seed film. All bicrystals viewed in this lattice image have been grown within the confines of a single Cr grain of the seed layer. However, the entire hard disk has a polycrystalline Cr layer with 2-D isotropy, and thus the polycrystalline Co layer is expected to have 2-D isotropy. Fig. 3b is an out-of-plane X-Ray Diffraction scan showing the $11\bar{2}0$ and 00.2 -Cr peaks indicative of the orientation relationship of these two films. (The larger peaks are due to the Al substrate and the broad hump is due to the amorphous Ni-P underplating; the Co and Cr peaks are small because the films are only 15 nm thick, even though both films are perfectly oriented.)

Fig. 3c is a BF-TEM view cross-sectioning the circumferential scratches, depicting the Co layer, the Cr seed layer and the amorphous Ni(P) plating beneath the Cr. (The base aluminum substrate beneath several microns of Ni plating is not viewed. A carbon overcoat protects the Co; and a Cap layer was applied for protection during TEM sample preparation.) On any one Cr grain, multiple bicrystals of Co can form, as indicated by the schematic. Electron diffraction (Fig. 3d) from the cross-sectioned TEM sample exhibits two strong reflections for the $11\bar{2}0$ and 200 planes parallel to the substrate in all grains of the Co and Cr films, respectively. These reflections are comparable to XRD rocking curves, with the narrow width of these reflections (as opposed to being arcs) indicating the relative goodness of film orientations. Additional reflections from cross-section electron diffraction correspond to planes perpendicular to the substrate that extend between Cr and Co films. The cross-section lattice image in Fig. 3e exhibits the closest-packed $\{011\}$ planes in the Cr seed layer extending to become the $\{1\bar{1}00\}$ planes in the Co film. In this particular Co grain the $\langle 0002 \rangle$ dipole is normal to the image, and thus along the texture scratches and parallel to the recording direction.

The crystallographic relationship that determines why $\langle 11\bar{2}0 \rangle$ Co film grows on a $\{200\}$ -Cr film is usually explained by a top-down template model of the last deposited atomic layer of the bottom film and the first atomic layer of the next layer.^{2,3,8,9} Templating is in essence a nucleation theory, even if/when it is just nucleating a new plane of the same material. Hetero-epitaxial growth (or nucleation) models typically present the surface as a template of filled atomic positions with the next layer to be deposited by filling empty positions (akin to stacking of oranges at the store). Thus the face of the unit cell of the nucleating film must match the face of the unit cell of the substrate, with some limited mismatch allowed. (Note that chemical limitations such as ionic repulsion are ignored because the media films are metallic alloys, but such could be accommodated by x - y spatial arrangements of ions.)

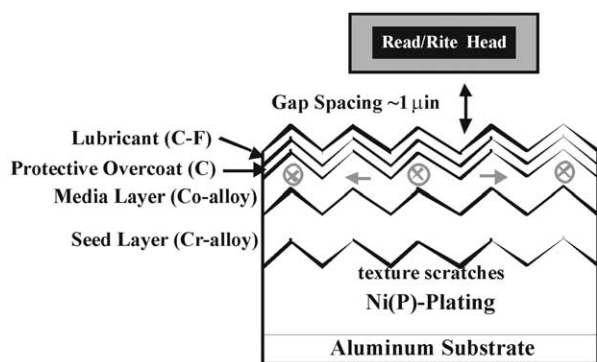


Fig. 2. Schematic of thin film magnetic media (not to scale) cross sectioning circumferential texture scratches. Longitudinal recording is enhanced if crystalline Co-dipoles align normal to section.

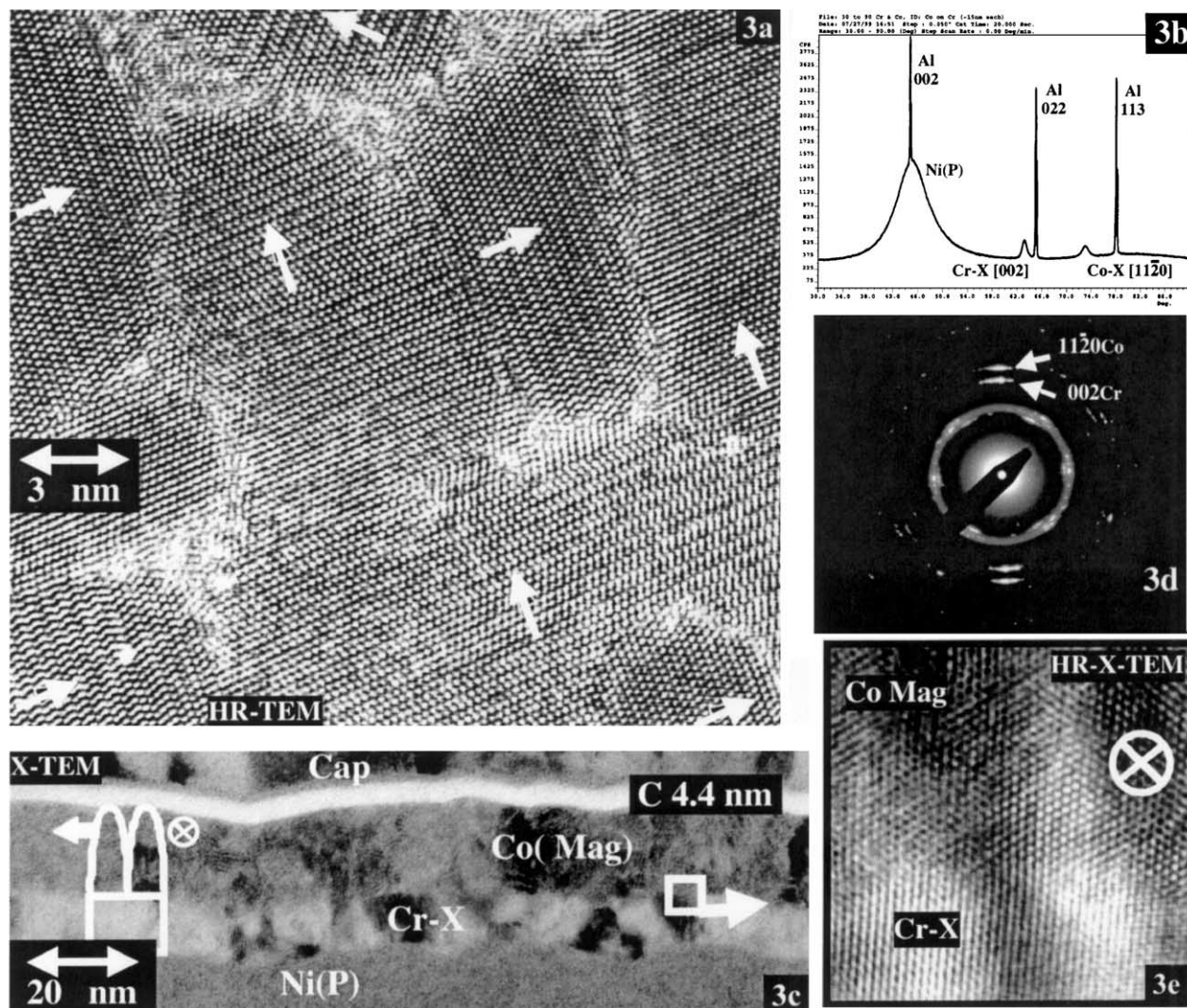


Fig. 3. (a) HRTEM of $11\bar{2}0$ -Co bi-crystals. (b) XRD of well-oriented Co and Cr thin films on an amorphous Ni(P)-plated, Al substrate. (c) Cross section TEM of media with schematic of 2 bi-crystals of Co growing on a $[200]$ -Cr seed grain. (d) SAD from X-TEM of well-oriented $11\bar{2}0$ -Co on 002 -Cr. (e) HRTEM from cross section depicting (110) planes of Cr extending to become (1100) planes of Co. $([0002]$ -dipole is normal to image.).

Fig. 4 is a schematic of a (200) cubic substrate with a square array of atoms on the surface, on which is deposited a $(11\bar{2}0)$ plane of a hexagonal material. Although this top film has a rectangular array, it is close to being a square array since the $1\bar{1}00$ and 0002 spacings are nearly equal. Yet more important for epitaxial growth, these spacings of the closest-packed-planes of the hexagonal film are nearly equal to the spacings of the closest-packed- (011) planes extending out of the cubic substrate. (Tailoring the Cr alloy can ensure the lattice of the seed layer enables a good epitaxial match for the subsequent Co-alloy media film.¹²) In addition, the templating can present the hexagonal array rotated 90° , indicating two bi-crystal orientations of the hexagonal Co could nucleate on each cubic Cr crystal with this $[200]$ orientation. Thus the template model is easily imagined in the HR-TEM lattice image of bicrystals in

Fig. 3a, where only one of the Cr- $\{011\}$ planes will match the 0002 planes in each Co bicrystal.

To consider a model different from templating, homoepitaxial nucleation is first considered, such as simple clean growth in an MBE process. A common model for this growth is the Terrace-Ledge-Kink (TLK) model³ (see schematic in Fig. 5a), where it is assumed there are always some ledges on any crystalline surface, and depositing ad-atoms have some mobility to move along a surface and finally attach at a ledge. Furthermore, the ad-atoms move along a ledge until they find kinks (or steps), where attachment to the ledge minimizes surface energy. (When the kinetic reactions are unfavorable for mobility of atoms to proper kink sites, epitaxial growth can be lost.) In Fig. 5a, the crystal growth direction is normal to the substrate and typically toward the direction from whence comes the source of

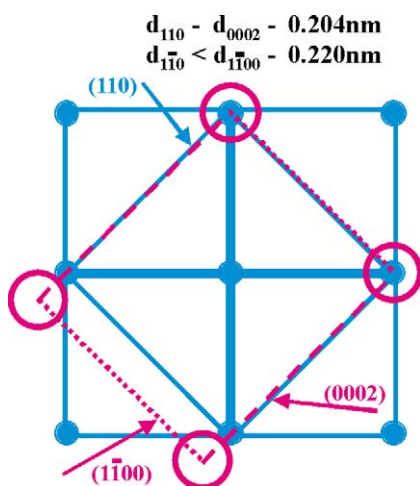


Fig. 4. Top-down template model of $11\bar{2}0$ -Co on 200-Cr.

ad-atoms. However, an interesting issue is that the fastest growing plane is the surface plane, which is extending itself parallel to the surface and normal to the macroscopic growth direction.

During many thin film growth processes, the surface is not as atomically flat as for an ideal MBE system; for example, the ion-sputter deposition of metallic films in this work. At any given juncture in the deposition process, the roughened surface can be envisioned as the other planes that are extending normal to the surface. Fig. 5b is a schematic where Fig. 5a has been rotated (counter-clockwise) 90° and the overall surface interface has been atomically roughened. It becomes naturally easier for these planes normal to the interface to grow upward toward the source of ad-atoms. In this process kinks and ledges are always available, as long as the flux of arriving atoms is high and even when the mobility of ad-atoms on surfaces is minimal. Growth becomes modeled as an extension of closest-packed planes normal (or near normal) to the surface; and the deposition of the next layer can become just a further extension of these same planes. In the cross-section lattice image of Fig. 3e, these planes (near) normal to the interface continue from the Cr seed layer into the Co media layer, with the (011) Cr planes becoming the $(1\bar{1}00)$ Co planes.

In an ideal system of epitaxy, the same crystallographic assessment should result from both the top-down template model (Fig. 4) with its corresponding monitor with out-of-plane XRD and the view of planes extending normal to the substrate (Fig. 5a) with the corresponding monitor of diffraction of such planes (by GIX or TEM). Thus it may appear the two models represent the same crystallographic interface control. In this work, however, diffraction from planes normal to the substrate provide a more thorough and more correct assessment of the crystallographic control at epitaxial interfaces. And in these fast-deposition systems, where interface roughness is common during growth, it is

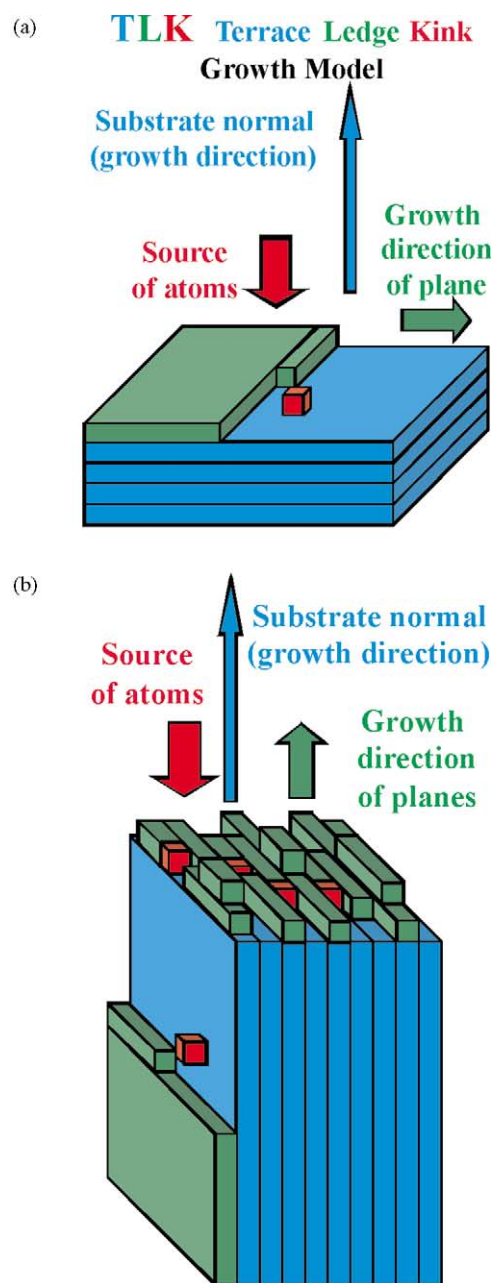


Fig. 5. (a) Terrace-ledge-kink model typical of epitaxial growth.^{2,3} Planes that are growing are actually extending parallel to the surface. (b) TLK rotated 90° so that growing planes extend normal to substrate. (caveat requires roughened surfaces as is typical for fast deposition processes.).

shown that a single set of normal planes (not the template model) can control the epitaxial growth.

When considering a template model as in Fig. 4, one is concerned with the planes parallel to the substrate, and a technique such as out-of-plane XRD (Fig. 3b) provides a monitor of goodness of orientations and consequently an indication of goodness of epitaxy. HR-TEM in plane-view (e.g. Fig. 3a) can visualize the template of one layer, but not both layers together. However, when considering the growth process as

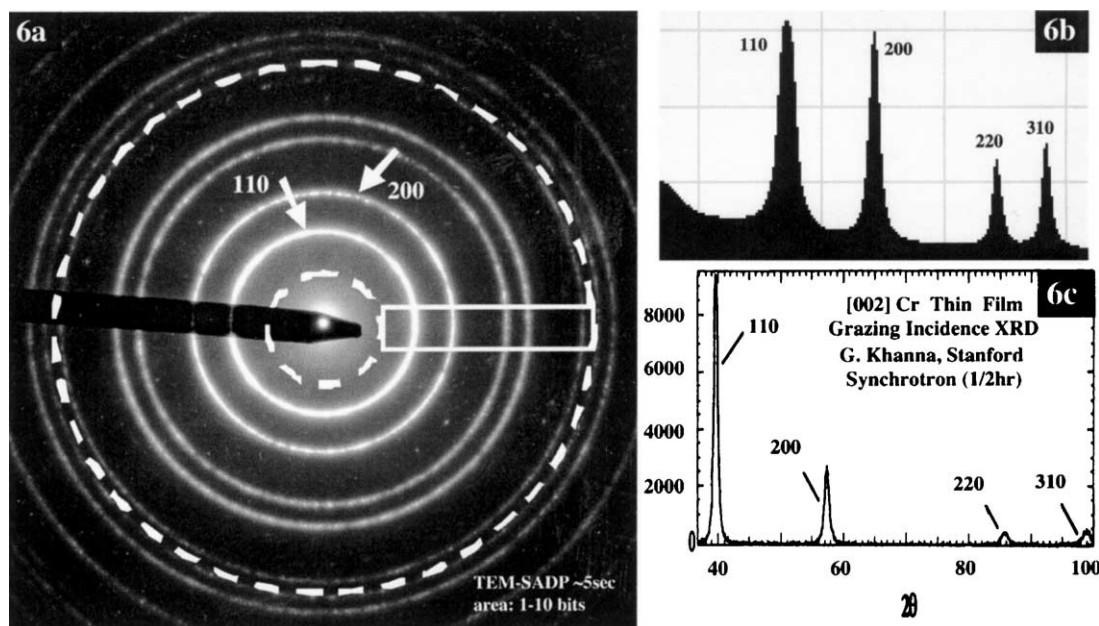


Fig. 6. (a) SAD ring pattern from plane-view TEM sample of 002-Cr thin film. (b) RA-radial averaging of SAD in (a). (c) GIX¹¹ of Cr film. The goodness of the 002 orientation is measured by the absent rings/peaks, such as 112.

depicted in Fig. 5b, the planes extending normal to the substrate become critical. Cross-section HR-TEM (e.g. Fig. 3e) does not study a statistically large portion of material, as well as having the difficulty of sample preparation. Thus a diffraction technique monitoring these planes is preferred. Grazing Incidence XRD (GIX^{2,10,11}) can provide a macroscopic measure of the planes normal to the substrate; however, the weak intensities from a thin film mean a high cost of analysis time and/or a synchrotron source of radiation.^{10,11} Electron diffraction performed on a plane-view TEM specimen monitors these same normal planes with statistically pertinent intensities obtained in a few seconds. Computer analysis of electron diffraction data has been developed^{12,13} to assist quantifying of different thin film samples.

Fig. 6a presents a ring diffraction pattern from a selected area (SAD) of ~500 nm diameter acquired of a Cr film grown with a [002] orientation but also having 2-Dimensional isotropy in plane. Whereas the out-of-plane XRD of Fig. 3b indicates one Cr peak for the [002]-oriented film, the electron diffraction of a plane-view sample has specific missing rings that indicate the film orientation. All rings correspond to planes belonging to the (002) zone, which means no diffraction from planes {hkl} with $l \neq 0$. Fig. 6b presents a computer radial averaging (RA) of the intensities of the diffraction rings of Fig. 6a. (Software is now a free plug-in available from NCEM/LBL for the Gatan Digital Micrograph program.) Fig. 6c is GIX data¹¹ obtained using synchrotron radiation source at SSRL. GIX samples the planes that are normal to the substrate, just as does plane-view electron diffraction, and thus the similarities in the peaks between the GIX data and the RA of

Fig. 6b. Besides the advantage of being more spatially discriminating and being a faster and less expensive acquisition, the ring diffraction data has the advantage of being able to simultaneously present possible circumferential differences in a single ring diffraction pattern. Conversely, the GIX analyzes orientations on only one planar cross section of the film, akin to measuring intensities of rings in electron diffraction by a single line trace crossing at a specific direction. To discriminate circumferential differences, the sample would have to be rotated and the GIX analysis would have to be repeated for each desired in-plane orientation.¹⁰ However, the GIX data can provide a more quantitative measure of intensities as long as sampling volume and uniformity of orientations through film thickness are kept constant. Since the intensities in electron diffraction can be affected by double diffraction, it is critical that thin areas of the TEM specimen are sampled. For the analyses of these thin films, the dynamical artifacts of diffraction can be minimized, and the intensities of the RA correlate well with GIX data.

One advantage of the electron diffraction data over the GIX can be the discrimination of different regions through the film thickness. Although grazing X-rays do not penetrate as deeply as traditional out-of-plane XRD, for thin films (< 100 nm in this work) GIX samples the entire thickness of the film(s). However, the preparation of TEM samples by thinning only from the backside produces a wedge-shaped sampling volume. The TEM can analyze just the topmost layers of a film, or the TEM can sample the entire thickness of the film. Thus electron diffraction in the TEM can differentiate crystalline changes through the thickness of a film as

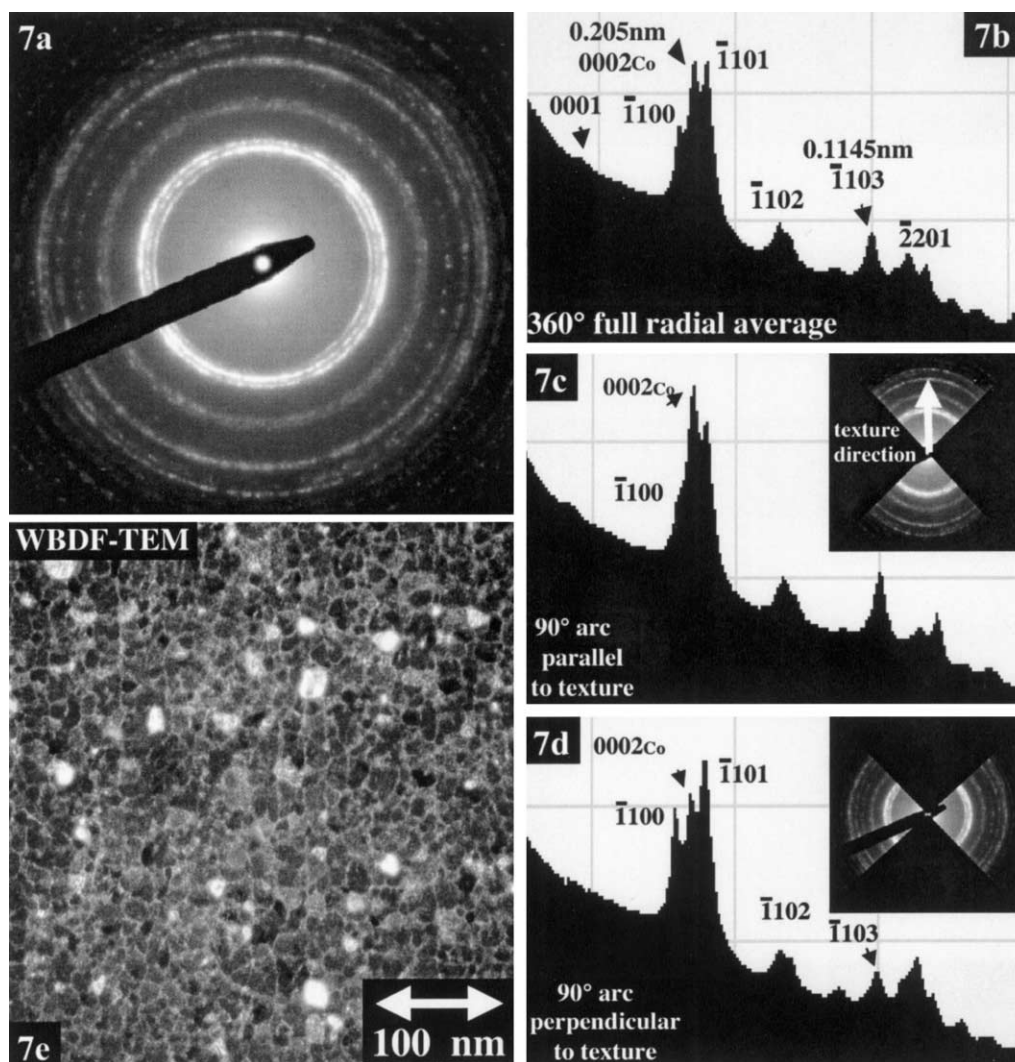


Fig. 7. (a) SAD ring pattern from plane-view TEM sample of 1120-Co. (b) RA of SAD rings with goodness of film orientation indicated by the absence of 1120 peak. (c) (d) RAs of sections, respectively parallel and perpendicular, to circumferential texture scratches. Relative peak intensities exhibit a strong preference of 0002 Co parallel to scratches. (e) Weak Beam Dark field of isolation between C-alloy grains.

compared to a singular analysis by XRD. In some cases, the orientation(s) can change as a film grows thicker; and it is the topmost atomic layer(s) of a seed layer that can control the growth of subsequent layers. Electron diffraction of a plane-view TEM specimen can definitively analyze just these topmost atom layers.

Fig. 7a presents a ring selected area diffraction (SAD) pattern from a region corresponding to a few bits of stored data of a Co film grown with a $[11\bar{2}0]$ orientation. At first glance, the rings appear to have circumferentially uniform intensities, which would suggest 2-Dimensional isotropy in-plane similar to the Cr film onto which the Co is grown. The Radial Average (RA) in Fig. 7b exhibits strong $1\bar{1}00$, 0002, and $1\bar{1}01$ intensities, and the negligible $11\bar{2}0$ peak indicates the goodness of the $11\bar{2}0$ growth orientation in the Co film. However, RAs exhibit different relative intensities when acquired of only sections of the ring diffraction pattern,

either parallel or perpendicular to the circumferential direction of the hard disk (Fig. 7c and d, respectively). A relatively strong 0002 peak, as compared to the $1\bar{1}00$ peak, is present in Fig. 7c indicating 0002 dipoles are preferentially aligned with the circumferential texture scratches. Conversely, the $1\bar{1}00$ peak is stronger in Fig. 7d indicating these planes are preferentially aligned parallel to the circumferential direction. Comparison to the relative intensity of the $1\bar{1}01$ peak provides a self-calibration for all RAs; however, such is not necessary because the $1\bar{1}01$ intensity is relatively constant in the circumferential direction. (The fanning effect¹⁴ is minimal in these films grown on surfaces with roughness of $R_a < 2$ nm.) With the establishment of different in-plane orientations by diffraction, corresponding Dark Field images can be generated from different in-plane g -vectors to study grain sizes.⁶ Weak Beam Dark Field (Fig. 7e) with TEM tilting toward $g = [0002]$ monitors

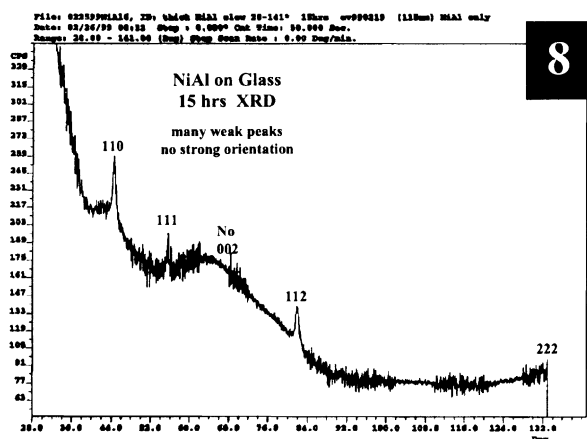


Fig. 8. XRD of thick NiAl, acquired with long duration and low noise, exhibiting most peaks (confirmed by GIX¹¹) and 3-D isotropy.

crystallographic isolation between grains comparable to EF-TEM monitoring of chemical segregation at grain boundaries.¹⁵ Fig. 3a exhibits bicrystals that form due to the multiplicity between the 4-fold 200 orientation of cubic Cr underlayer and the 2-fold 1120 orientation of the hexagonal Co layer. However, the scratches enable an anisotropic relaxation in the Cr {011} plane spacings such that the 1100 planes of Co epitaxially prefer to align parallel (or near parallel) to the texture scratches. Thus an ideal polycrystalline Co film is produced with circumferentially-oriented magnetic dipoles and 1.5-dimensional crystallography.

2.2. Part II Co-alloy/Cr/NiAl/polished-glass-substrate; reduction from 3-D-isotropy to 2- & 1/4-D

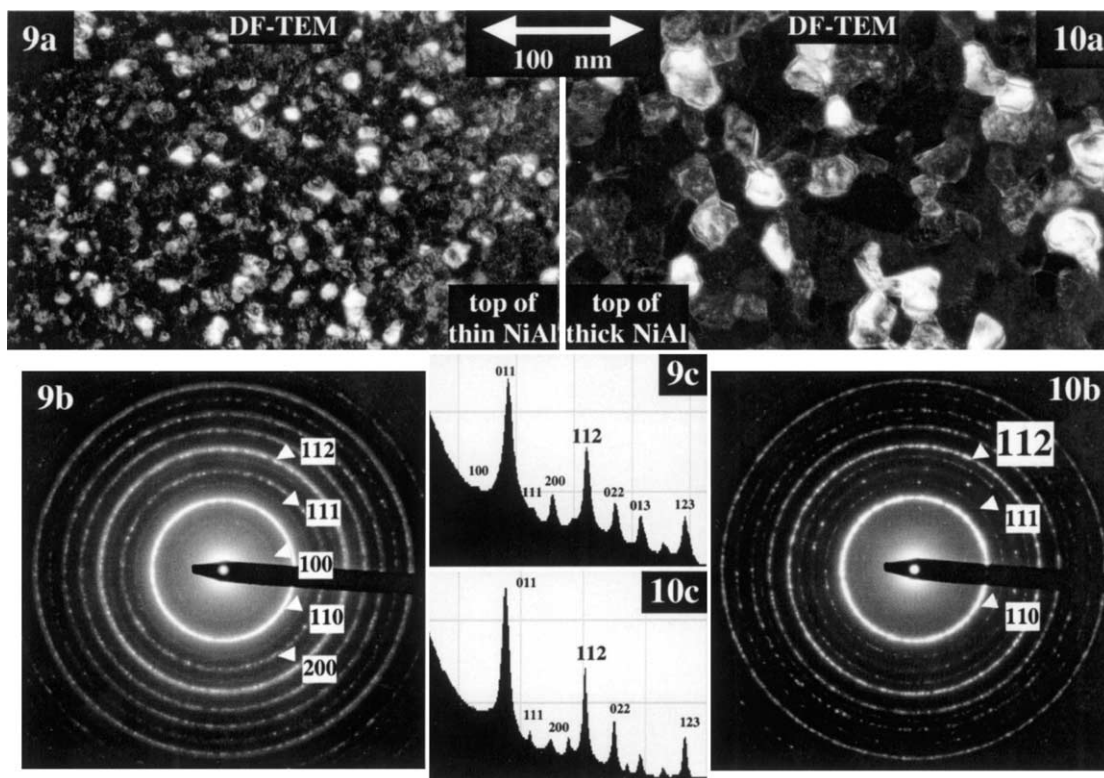
The thin films described in the second part of this work have been developed for a different information storage requirement, in particular media utilized in hard drives for portable computers. In this system there is no scratch texture, as such is not needed to prevent tribological stiction between the head and media. However, the requirements of impact resistance and thin formfactor have led to the utilization of glass substrates (as opposed to traditional nickel-plated aluminum substrates in Part I). The sputter deposition of Cr onto glass substrates does not provide a uniform small grain size, and a sub-seed layer of NiAl has been deposited first to provide a small grain size. Small grain size in the seed layer(s) ultimately develops a small Co grain size, which in turn is necessary to optimize high-density storage.^{6,8,16–18} (The schematic of cross-sectioned films in Fig. 12 differs from Fig. 2 with an additional sub-seed layer of NiAl and without texture scratches.) NiAl has become a desirable layer because it has a d-spacing for (110) planes that is essentially equal to that of Cr, which then matches the Co d-spacings. Other published studies

have characterized the NiAl films as developing a $\langle 112 \rangle$ crystallographic orientation and have determined a template relationship between 112-cubic and 1100-hexagonal to provide longitudinal media with $\langle 0002 \rangle$ dipoles in the plane of the film.^{17,18} However, this present work does not reveal a $\langle 112 \rangle$ NiAl orientation, and as in Part I prefers planes-extending (near) normal to the interface rather than templating as a model for crystallographic control at interfaces.

An out-of-plane XRD scan is presented in Fig. 8 of a relatively thick (~ 115 nm) NiAl film sputter-deposited onto a glass substrate. Specific angular regions where peaks are expected have had extended scan durations (of 0.0004° per second to improve signal-to-noise. If the entire scan had been performed at $0.0004^\circ/\text{s}$, it would have required several days for acquisition.) This XRD scan was performed on a Scintag Diffractometer, which uses a solid-state detector that reduces the noise level and enables small signals to be detected for 111, 222, and other peaks (confirmed by synchrotron XRD¹⁰). In other reports,¹⁷ XRD has observed 110 and 112 as the strongest peaks. The 110 peak is the first to be observed for the thinnest NiAl films because the 110 is the naturally most intense X-ray peak for cubic NiAl. As NiAl films grow thicker, the 112 peak is also observed, but the intensity of the 110 peak does not continue to increase proportionally with thickness. This indicates a change in average orientations for thicker films. However, the earlier report¹⁷ had insufficient signal-to-noise to detect the other XRD peaks detected in this present study. In addition to XRD intensities being weak due to film thinness and not being singularly oriented, the peaks are also broadened by the fine grain size of the NiAl. Thus a TEM study of thin and thick NiAl films provides a more thorough understanding with imaging of grain sizes and electron diffraction of orientations.

Dark Field imaging acquired of a plane-view TEM sample of a thin (~ 20 nm) NiAl film exhibits a grain size < 10 nm (Fig. 9). The sample has been prepared by removing material only from the substrate side of the sample. This enables the TEM sampling area to be a wedge-shape, where the thinnest areas of the sample represent just the topmost atom layers of the NiAl. When moving to thicker regions of the TEM sample, multiple grains overlap each other in the TEM projection, which indicates the grains do not grow perfectly columnar. Consequently, the image of Fig. 9 is acquired in the thinnest regions of the TEM sample to illustrate the grain size at the topmost of the layer.

Fig. 9 is a ring diffraction pattern acquired of an 800 nm-diameter region of the film imaged in Fig. 9. Fig. 9 presents the radial average (RA) of the diffraction ring intensities, with the presence of all peaks indicating no singular growth orientation has developed in the thin film. Although the 100 is a naturally weak intensity in the B2-cubic NiAl structure, it appears weaker than



Figs. 9 and 10. (9a) Dark Field TEM image of NiAl grains at the top of a thin (~ 20 nm) film. (b) SAD ring pattern from plane-view TEM specimen. (c) Radial average of SAD showing all rings. (10a) DF-TEM image of NiAl grains at the top of a thick (~ 80 nm) film. (b) SAD ring pattern from same area. (c) RA exhibiting weaker 100 and 200 peaks; however, strong 112 peak in-plane means no predominant 112 orientation out-of-plane.

expected indicating the film is not fully 3-dimensionally isotropic. When moving to the thicker regions of the TEM sample where additional smaller grains are observed, the 100 intensity increases relative to other peaks. Since the entire NiAl film thickness is much less than that needed to cause significant double diffraction, the change in relative peak intensities indicates the film orientation is more random at the bottom of the film than at the top.

A thicker (~ 80 nm) NiAl film exhibits a larger grain size when imaged by Dark Field plane-view TEM (Fig. 10a). Again the TEM specimen is prepared by only removing material from the backside, and again this TEM sampling area represents the grain size at the top of the NiAl film. As compared to Fig. 9a, the grain size increased more than 5-fold; although it is noted that the grain sizes in both films are smaller than the thickness dimension of the film. Also when moving to thicker regions of the TEM sample, many more overlapping grains are observed indicating the grains are not growing perfectly columnar. Only some of the small grains, viewed in Fig. 9a when the film is thin, continue to grow to become the large grains viewed in Fig. 10a when the film thickens. An opposite view, which is deduced by the following diffraction data, is that most of the small grains die out as the NiAl film thickens.

Fig. 10b is the ring diffraction from the topmost of a thicker (~ 80 nm) NiAl film, and Fig. 10c is the corresponding RA of the intensities. As compared to Fig. 10c, the intensity of the 200 peak has weakened, and the intensity of the 100 peak has become negligible. However, this combination of rings does not represent planes that all belong to a single zone, and thus no singular orientation has developed at the top of the thick film. Other reports have claimed that the observation of a 112 peak in XRD data indicates NiAl grows with a $\langle 112 \rangle$ preferred orientation.^{17,18} However, an electron diffraction pattern acquired along a $\langle 112 \rangle$ orientation would not exhibit 112 reflections. Thus the presence of $\{112\}$ planes extending normal to the substrate is an indication that there is not a preferred $\langle 112 \rangle$ growth normal for the thicker NiAl film.

Although there is no singular preferred orientation developing as the NiAl film thickens with grain size increasing, there are specific orientations that are being lost. As the 200 ring disappears for thicker films, it indicates crystal orientations having 200 planes in their zone are also disappearing. This means the top of the thick film has no grains oriented along $\langle 001 \rangle$, $\langle 011 \rangle$, $\langle 012 \rangle$, etc. This is consistent with the out-of-plane XRD observations that the 011 peak intensity does not continue to intensify as the film thickens.

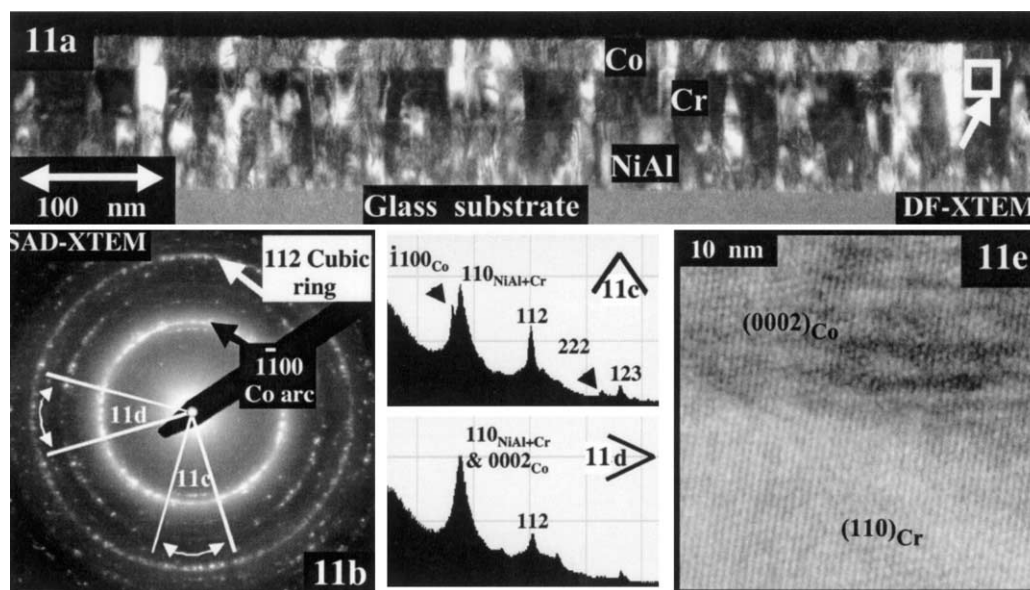


Fig. 11. (a) Cross section DF-TEM image depicting NiAl and Cr seed layers with top Co media. (b) SAD from X-TEM, with continuous 112 ring indicating no orientation preference. However, gaps exist in the 200 ring; and $\bar{1}100$ -Co exists only over an arc of $\pm 20^\circ$ from substrate normal. (c) (d) RAs of sections of SAD, out-of-plane and in-plane, respectively. (e) HRTEM exhibiting closest packed planes of seed layer extending to become close-packed planes of media layer. Planes are not normal to substrate because no preferred orientation is present.

Grains with $\langle 011 \rangle$ orientations exist at the bottom of the film, but these grains grow slowly and are overgrown by other grains. Similarly, the $\langle 001 \rangle$ growth orientations die away even before the $\langle 011 \rangle$ (and the weaker 001 peak is never observed by XRD in the thinner films). A loss of specific orientations, however, does not result in the development of a singular growth orientation, at least not until the grain size would have grown so large that it would be of no practical use as a seed for high-density storage media.

One approach to showing that grains grow larger as the film thickens is to provide a cross section view, as depicted in Fig. 11a. However, for very small grain sizes, the TEM cross section view can be misleading and an interpretation of Fig. 11a would suggest columnar growth of grains with minimal increase in grain size with thickness. In contrast, comparison of the two plane-view images (Figs. 9a and 10a) demonstrates the dramatic increase in grain size as the film thickens. Cross section TEM samples can have two major drawbacks, poor sampling statistics and a specimen thickness that leaves many overlapping grains. The cross-section TEM sample ends up with very little sampling area because of dissimilar thinning of the film(s), substrate, and preparation materials such as glue. In comparison, the plane-view sample provides a more statistically correct measure of grain size and orientations. Also most cross section specimens are < 20 nm thick for most of the imaging area. When grain sizes are small (< 20 – 40 nm) this means the majority of the imaged cross section actually has overlapping grains. Thus it becomes difficult to assess how columnar the grain growth truly is.

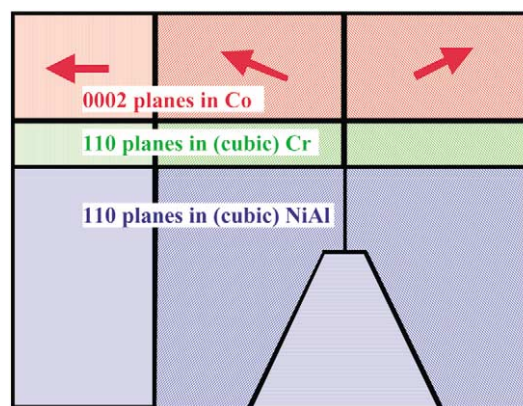


Fig. 12. Schematic cross section of Co thin film grown on Cr and NiAl seed layers. NiAl grain size grows as film thickens by low-energy facet-terminated grains dying out. (110) planes of NiAl intersecting surface (near) normal extend to become close-packed planes in Cr, which in turn extend to become (0002) planes in Co. Co-[0002]-dipoles lie $\pm 20^\circ$ of in-plane; however for thinner films, shape anisotropy pulls dipoles more in-plane.

The cross section image (Fig. 11a) has dramatic impact, especially with dark field contrast showing the crystallographic alignment between grains of each layer, from NiAl to Cr to Co. But as a monitoring tool of grain size development, it may not provide the quantitative analysis that two plane-view images provide.

Similar to imaging, the electron diffraction from a cross-section sample may not be as easily quantified and does not provide the desirable sampling statistics as does electron diffraction from plane-view samples. However, the cross section diffraction (Fig. 11b) of the

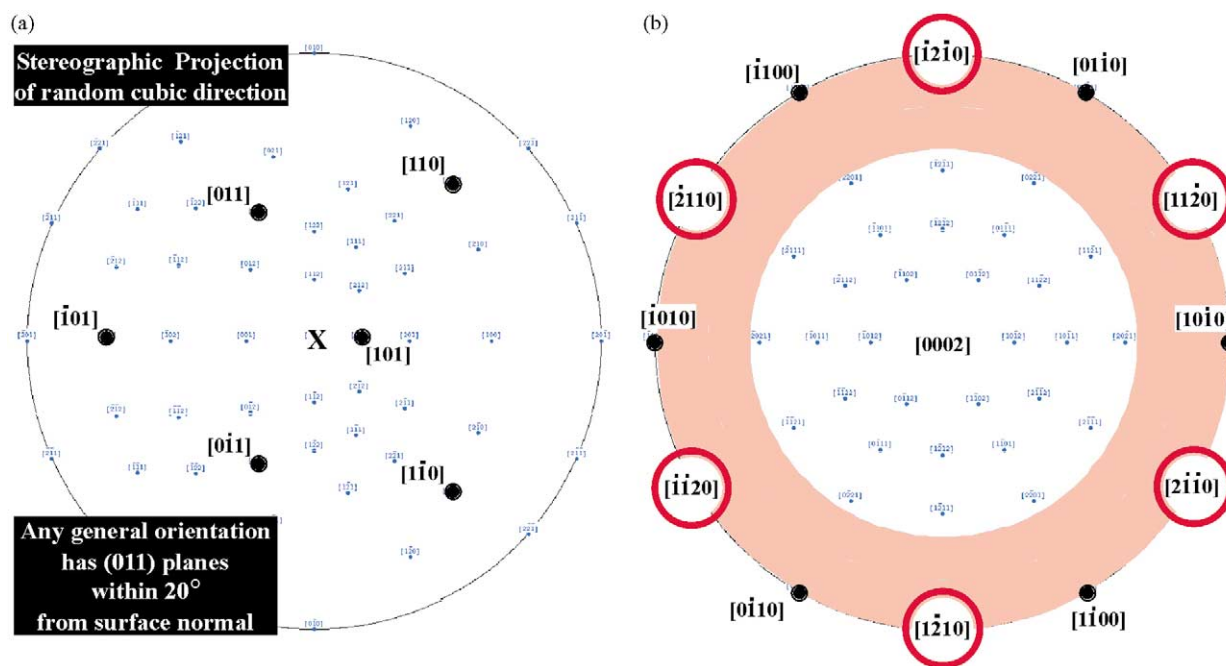


Fig. 13. (a) Stereographic projection of cubic seed layer exhibiting multiplicity of $\{110\}$ planes. For any randomly oriented grain, a set of $\{110\}$ planes will intersect surface within $\pm 20^\circ$ of normal. These planes become the $\{0002\}$ planes in Co, and $\{0002\}$ dipoles will be $\pm 20^\circ$ from lying in-plane. (b) Stereographic projection of hexagonal $\{0002\}$. The banded region of $\pm 20^\circ$ represents possible grain orientations which have $\{0002\}$ dipoles nearly in-plane. Since $11\bar{2}0$ -Co grows on 200-cubic, and the 200-cubic died out early in the NiAl film, then $11\bar{2}0$ orientations are absent “holes” for the Co. Thus the only major peak observed out-of-plane for the Co is $1\bar{1}00$.

NiAl/Cr/Co-alloy films does exhibit both the 3-dimensional isotropy for the cubic seed layers, as well as the reduction of orientations in the hexagonal Co media. In comparison, Fig. 11b exhibits many continuous rings versus the strong singular reflections observed in cross section of Cr/Co of Fig 3d. Whereas Fig. 3d represented well-oriented $[200]\text{-Cr}/[11\bar{2}0]\text{-Co}$ films, the rings in cross-sectioned NiAl films indicate random orientations out-of-plane. If NiAl (and the subsequently deposited cubic-Cr layer) had a $\{112\}$ orientation as reported by XRD,¹⁷ then the electron diffraction in Fig. 11b would exhibit a singular 112 reflection instead of the continuous 112 ring. Having a continuous 112 ring in cross section, as well as a continuous 112 ring in plane-view (Figs. 9b and 10b) is an indication of 3-dimensional isotropy;...at least as regards to the orientation of 112 planes.

Not all rings in the cross section electron diffraction are observed and/or continuous. The 200 cubic ring, for example, is absent both perpendicular and parallel to the substrate, thus leaving stronger intensities at the 45° angles. This does not represent a favoring of 200 orientations at 45° to the film, but rather just means an absence of 200 orientations normal to the substrate. The missing 200 reflections normal to the substrate confirms the XRD (Fig. 8) observing no 200 reflection, and the missing 200 reflection in the plane of the film is consistent with the plane-view diffraction (Fig. 10b) observing no 200 ring. Fig. 11c and d are RAs, perpendicular

and parallel to the substrate respectively, that contrast the varying intensities within the diffraction rings of Fig. 11b. The dominant peak in both RAs corresponds to the d-spacing of 110-cubic and 0002-hexagonal, and this overlap hinders a quantitative interpretation of preferences in these plane orientations. However, Fig. 11c does exhibit a peak corresponding to the $1\bar{1}00$ -hexagonal orientation, indicating this orientation of the Co media is predominantly normal to the substrate. Fig. 11b shows this $1\bar{1}00$ ring exists only as an arc $\pm 20^\circ$ from normal to the substrate; but the arc has a relatively uniform intensity indicating a range of orientations without a special preference within that range. (Typically an XRD rocking curve of a partially oriented film is expected to exhibit a higher intensity directly normal than at a few degrees from normal.) Fig. 11e is a HR-TEM image exhibiting the lattice fringes as they pass from being (110) planes in the cubic seed layers to being (0002) planes in the hexagonal-Co media. Since most grains in the films do not have an exact normal orientation, these planes typically intersect the interface somewhat off normal even though the substrate surface is flat (see Fig. 11a).

A preferentially oriented Co- $1\bar{1}00$ film grown on a 3-dimensionally random arrangement of cubic-112 orientations seems confusing as justifying an epitaxial interface. Furthermore, it bodes poorly as a representation of a template crystallographic relationship of hexagonal- $1\bar{1}00$ and cubic-112, as has been previously

interpreted from XRD data.^{17,18} However, rather than interpreting the 1100 arc in Fig. 12b (or $1\bar{1}00$ peaks in XRD¹⁷) as a preference of orientation, it can be viewed instead as only a loss of $1\bar{1}00$ in all other directions. This is akin to the above analyses of the missing portion of cubic rings as meaning only missing orientations, not any preferred orientations. Thus without being able to declare a singular growth orientation, it becomes difficult to justify a specific templating model.

Since a $1\bar{1}00$ -hexagonal-on-112-cubic template model is not warranted by the continuous rings in electron diffraction, a model is presented again like that of Part I to describe epitaxy via extension of close-packed planes between layers. Fig. 12 is a schematic cross-section of NiAl seed layer, a subsequent Cr-alloy-seed layer, and a top Co-alloy media layer. Within each grain of each polycrystalline film is drawn one set of closest packed planes (e.g. the $\{110\}$ -cubic planes and the $\{0002\}$ hexagonal planes). As the NiAl layer grows thicker, the grain size increases (as observed in Figs. 9a and 10a) because some grains have slow-growing NiAl orientations. For example, when a NiAl grain has its $\{110\}$ plane parallel to the surface, its surface energy is minimized when that close-packed plane is kept flat. Then depositing atoms will preferentially move to the roughened surfaces of neighboring grains. The neighboring grains eventually grow over, not because these neighboring grains have fast-growth orientations, but rather because the $\langle 110 \rangle$ -oriented grain is growing slowly. After growth of a modestly thick NiAl, electron diffraction and XRD showed that the $\langle 110 \rangle$ -oriented grains had died, as well as $\langle 100 \rangle$ oriented grains. Yet the average NiAl grain retains a 3-D-random orientation at the top surface. The subsequent seed layer of Cr retains the same cubic orientation as has each grain of NiAl beneath it; with the advantage that alloying the Cr can subtly modify the d-spacings. Although the grain size continues to grow as the Cr film thickens, the average Cr grain also has a 3-D-random orientation at the top surface. This means each grain will have its closest-packed $\{110\}$ planes intersecting the surface at some oblique angle. These planes extend into the depositing Co to become (0002) planes, thereby causing the $\{0002\}$ planes, and the corresponding magnetic dipoles to be at an angle.

Stereographic projections are used to show why the cubic seed layers have grains with 3-D-random orientations, yet the hexagonal Co media exhibits only a limited range of orientations. Fig. 13a is a cubic stereographic projection (with the poles representing planes) that has been rotated to a random orientation to represent the orientation in a typical random grain of the cubic seed layer. Because of multiplicity of the cubic structure, there are six $\{110\}$ -type planes. For any random orientation, there will be at least one set of $\{110\}$ planes that intersects the surface within $\pm 20^\circ$ of

normal. It is these closest-packed planes that continue growing as the next layer; NiAl- $\{110\}$ planes continue to become Cr- $\{110\}$ planes, which continue to become Co-(0002) planes. Thus Co grains only have orientations which have the (0002) intersecting within $\pm 20^\circ$ of normal.

Fig. 13b is the hexagonal stereographic projection oriented along the 0002 orientation. And a banded region is drawn 20° away from the great circle perimeter. All orientations within this band have their (0002) plane intersecting the surface within $\pm 20^\circ$ of normal. This includes only two of the major low index zones for the hexagonal structure: $\langle 1\bar{1}00 \rangle$ and $\langle 1120 \rangle$. As noted in Part I, the $\langle 1120 \rangle$ -hexagonal orientation nucleated on the $\langle 200 \rangle$ -cubic; however, the $\langle 200 \rangle$ orientation died out early in the NiAl growth. Thus without $\langle 200 \rangle$ -cubic oriented seed grains, the $\langle 1120 \rangle$ -hexagonal orientation is singularly missing. Thus the banded region of allowable orientations in Fig. 13b has absent poles (holes) indicating $\langle 1120 \rangle$ orientations are not present in the Co. This results in $\langle 1\bar{1}00 \rangle$ as the only major orientation in the Co media, consistent with observations by electron diffraction (Fig. 11b) and XRD.¹⁷

Since these $\langle 1\bar{1}00 \rangle$ orientations are spread over a $\pm 20^\circ$ range, this means few of the 0002-magnetic dipoles lie exactly within the plane of the longitudinal media. The cones of allowable orientations produce dipoles with 2- $\frac{1}{4}$ -dimensional isotropy. Without the dipoles lying in the plane of the film, this would seem to bode poorly for longitudinal media. However, the final shapes of the Co grains can have an additional impact. Since modern media films are quite thin (< 10 – 15 nm), then the grain thickness can be less than the grain size. Such a squat shape, as depicted in Fig. 12, causes the dipoles slightly out-of-plane to be pulled into plane by forces of magneto-shape-anisotropy. As future hard drives require thinner media, the grain shape will make the media dipoles come closer to 2-D isotropy.

3. Conclusions

A model for plane extension (Fig. 5b) rather than a template model (Fig. 4) can be used to interpret the epitaxial control at interfaces both for well-oriented (Part I) and nearly random (Part II) films. This model indicates that a single set of closest-packed planes that intersects the surface is dominant in seeding the growth of a set of planes in the next layer, with these planes extending across the interface. Since fast deposition processes have naturally rough terminations, these extending planes provide a large source of “kink” sites, and planes get to grow (extend) in the direction toward the atom sources. Once atoms impinge the surface, they do not have to diffuse far to find kink sites. In a fast

deposition process, this becomes critical for retaining epitaxial growth.

Judicious choice and processing of a Cr-alloy seed layer film can establish a polycrystalline film with 2-D isotropy and a [200] growth texture normal to the substrate. However, subsequent deposition of hexagonal Co-alloy media can be reduced to 1- $\frac{1}{2}$ -D isotropy. Furthermore, alignment of Co- $\langle 0002 \rangle$ dipoles in the circumferential direction aligns the magnetic dipoles with the magnetic fields of the write/read head, thereby enhancing longitudinal properties.

For Co films growing on randomly oriented NiAl, the matching of one plane spacing in the lower layer to a plane spacing in the depositing film is the predominant requirement for epitaxy. The inverse multiplicity between cubic-seed-layer and hexagonal-Co-layer leads to reduction in orientations. The 2- $\frac{1}{4}$ -D isotropy in Co media on 3-D-isotropic NiAl enhances longitudinal recording, and the fine grain size improves signal-to-noise of thin film media.

Acknowledgements

The authors gratefully thank the employees of Komag Inc., Stanford University, and NCEM/LBL for their respective help in processing materials, use of TEM, and development of computer algorithms.

References

1. <http://www.research.ibm.com/research/gmr/basics.html>.
2. Ohring, M., The materials science of thin films. *Academic Press*, 1992, 307–350.
3. Tiller, W. A., *The Science of Crystallization*. Cambridge Press, 1991.
4. Hinderberger, S. and Dahmen, U., Growth and TEM characterization of heteroepitaxial thin metal films. *MRS Proceedings*, 1997, **472**, 27–33.
5. Dahmen, U., Structure and symmetry of multicrystal thin films grown on single crystal templates. *Boundaries and Interfaces in Materials, TMS*, 1998, 225–235.
6. MoberlyChan, W. J., Dorsey, P., Nolan, T., Alex, M. and Yamashita, T., TEM to support magnetic media development in YR2000. *Mater. Res. Soc. Symp. Proc.*, 2000, **614**, 331–336.
7. Nolan, T. P., Sinclair, R., Ranjan, R. and Yamashita, T., Effect of microstructural features on media noise in longitudinal recording media. *J. Appl. Phys.*, 1993, **73**(10), 5567–5571.
8. Nolan, T. P., *Effects of Microstructure and Crystallography on the Magnetic Properties of Recording Media*. PhD thesis, Stanford University, 1994.
9. Johnson, K. E., Mirzamaani, M. and Doerner, M. F., In-plane anisotropy in thin-film media: physical origins of orientation ratio. *IEEE*, 1995, **26**(6), 2721–2728.
10. Khanna, G., *Structural and Magnetic Characterization of Longitudinal Recording Media*. PhD thesis Stanford University, 2001.
11. Khanna, G. and Clemens, B., *J. Appl. Phys.* (submitted for publication).
12. MoberlyChan, W. J., Kilaas, R., Chan, L. H., Nolan, T., Dorsey, P., Cao, W., Lu, M., Gopal, M. and Yamashita, T., Computer analysis of electron diffraction from thin films. *Microscopy*, 1998, **4**(2), 344–345.
13. MoberlyChan, W. J., Dorsey, P., He, L., Zhang, M., Lairson, B. and Lu, M., TEM & computer analysis of crystallographic orientation ratio in [1120]-Co films on [002]-Cr films grown on mechanically textured substrates. *Microscopy*, 2000, **6**(2), 956–957.
14. Kataoka, H., Bain, J. A., Brennan, S. and Clemens, B. M., Crystallographic anisotropy in thin-film magnetic recording media analyzed with X-ray diffraction. *J. Appl. Phys.*, 1993, **73**(11), 7591–7595.
15. Thomas, G. and Goringe, M. A., *Transmission Electron Microscopy of Materials*. J. Wiley Publ., 1979.
16. Wittig, J. E., Nolan, T. P., Sinclair, R. and Bentley, J., Chromium distribution in CoCrTa/Cr longitudinal recording media. *Mater. Res. Soc. Symp. Proc.*, 1998, **517**, 211–216.
17. Zou, J., Laughlin, D. and Lambeth, D., CoCrTa intermediate layers on NiAl underlayers for CoCrPt longitudinal thin film magnetic media. *IEEE Trans. Magn.*, 1998, **34**(4), 1582–1584.
18. Bian, B., Bain, J. A., Kwon, S.-J. and Laughlin, D. E., High coercivity Co-alloy thin films on polymer substrates. *IEEE Trans. Magn.*, 2001, **37**(4), 1640–1641.